2025 IEEE World Haptics Conference (WHC)
Suwon Convention Center, Suwon, Korea
July 8 ~ 11, 2025

Textured Phantom Sensations: Rendering Spatial Textured Signals between Fingertips Using Vibrotactile Phantom Illusion

Minwook Lee
Department of AI Convergence
Gwangju Institute of Science and Technology
Gwangju, South Korea
minwook-lee@gm.gist.ac.kr

Hasti Seifi
School of Computing and Augmented Intelligence
Arizona State University
Tempe, Arizona, United States
hasti.seifi@asu.edu

Gunhyuk Park
Department of AI Convergence
Gwangju Institute of Science and Technology
Gwangju, South Korea
maharaga@gist.ac.kr

***Abstract*—Phantom sensation (PS), an illusory sensation occurring between multiple stimulated sites, has been used to deliver spatial information with simple sinusoidal vibration signals, offering limited expressivity for haptic design. To address this limitation, we assessed the robustness of PS to complex waveforms of texture vibrations delivered to the index and middle fingertips, which we refer to as textured PS (TPS) for brevity. In Study 1, we investigated spatially static and dynamic PS with temporally stationary texture vibrations from three textures. Study 2 examined both spatially static and dynamic PS for five temporally nonstationary texture vibrations generated from two scratching motions. Average texture recognition accuracies for temporally stationary vibrations were 57.6% and 59.7%, while those of temporally nonstationary vibrations were 67.5% and 72.4% for spatially static and dynamic TPS, respectively. Our work extends PS to deliver spatial information with complex vibration waveforms while maintaining comparable performance to simple sinusoidal PS. We discuss the implications of our work for designing expressive phantom vibrations in user applications.**

***Index Terms*—Phantom Sensation, Complex Waveform, Texture Vibration, Spatial Accuracy, Texture Identification**

I. Introduction

The vibrotactile phantom sensation (PS), a single illusory vibration felt between multiple stimulation sites, has been widely used to provide spatial information on various body sites using multiple vibration actuators. After the pioneering work by Alles [1], PS has been investigated in connected body sites [2], [3], penetrating body [4], and out-of-body sensations [5]. These studies have provided quantitative assessments of the spatial performances in delivering single location [5] and moving PS [6]. PS has been primarily reported for single-frequency sinusoidal vibrations, and recent attempts validated its illusion for different frequency vibrations [7], [8].

Meanwhile, vibration patterns can deliver diverse information with realistic or abstract meanings. For realistic vibration patterns, the most common approach is mimicking the signals generated from real-world events such as vibrations from scratching a real-world texture with a pen [9] and decaying exponentials for collisions [10]. Additionally, researchers have designed vibration patterns to provide perceptual roughness [11] or convey abstract information [12], metaphors, and emotions [13], [14]. These vibrotactile signals convey rich and nuanced sensations through complex signals that vary in amplitude and frequency. Yet, these complex waveforms have not been used together with the PS illusion.

To address this gap, we propose textured phantom sensation (TPS), a vibrotactile texture illusion occurring between the index and middle fingertips. As an extension of PS, TPS substitutes the carrier waveform with the texture vibration signal to enable the design of expressive haptic effects for user applications. TPS merges the strengths of PS and vibrotactile feedback, where PS mainly affects user experience by co-locating the event and feedback sites, and vibrotactile feedback focuses on improving realistic sensation by providing appropriate temporal waveforms. Thus, TPS can be useful in applications where both spatial and detailed temporal information are important. For instance, TPS can enable designers to simulate the flow of various liquids, gases, and small particles (e.g., a sandstorm) on a user's hand in a virtual reality (VR) science education scenario. With TPS, designers can also create diverse realistic and magical effects (e.g., a virtual slingshot) between the user's fingers during a VR experience or video game. Prior work has shown accurate transmission of spatial [15] information can enhance user experience, which suggests the utility of TPS. Yet, little is known about how accurately users can perceive the phantom sensations and complex waveforms with TPS.

To assess the efficacy of TPS, we ran two user studies evaluating user performance in recognizing both spatial (location, movement) and spectral (texture) information with TPS. In User Study 1, we validated TPS for three stationary texture waveforms (nylon bag, ABS plastic, terra-cotta) with three rendering methods (linear, logarithmic, energy). Stationary vibration refers to a waveform with a constant amplitude generated by a controlled motion input. We assessed the spatially static TPS with five intended locations (*L1-L5*; *L1* and *L5* denote the index and middle fingertips, respectively) and the dynamic TPS using two movement directions (*L1 to L5*, and *L5 to L1*). In User Study 2, we assessed TPS for five temporally nonstationary texture waveforms (nitrile gloves, microfiber clothes, aluminum, artificial grass, and sandpaper aluminum oxide) generated from two input scratching motions (*Slow* and *Fast*) for the same spatial conditions on both the spatially static and dynamic TPS. In both studies, TPS could deliver spatial and texture information in both spatially static and dynamic rendering with user performance (error, motion slope) comparable to the simple sinusoidal phantom sensations in prior work. Also, we showcased our proposed TPS in two demonstrations: (a) during live scratching of real textures with a pen stylus and (b) in a brick-breaker game application in two haptics conferences and collected user comments. Finally, we ideated a set of scenarios for TPS in user applications. In summary, we showed that textured phantom sensations can deliver spatial and texture information at a single target location and along a moving trajectory between fingertips. In the following sections, we provide related literature, an explanation of our texture signal design, two user studies on temporally stationary and nonstationary textured phantom sensations, and implications of the results.

II. Related Work

In this section, we discuss previous literature on vibrotactile information and phantom sensation.

A. Vibrotactile Information

Vibrotactile feedback is often used for information delivery in various applications. Prior work has investigated various applications such as driving a vehicle [16], tele-operation [17], or virtual environments [18]. In applications requiring high realism, a common approach involves capturing vibrations from real-world physical interactions and playing the vibration signals using wide-band actuators. For example, the record-and-play of accelerations has increased the realism of kinesthetic force-feedback systems in surface interactions [19] and surgical procedures [20]. Another approach is converting sound waveform into vibrotactile signal by shifting their frequency bandwidth into the perceivable frequency range of vibrations [21], mapping perceptual parameters between the auditory roughness and loudness to the tactile dimension [11], or applying the exponential decay from impulse collision sound to sinusoidal vibrations [22]. Also, Kuchenbecker et al. proposed a linear prediction model to reproduce texture vibrations from physical interactions between a pen and diverse real-world textures [9]. This approach was later extended to the Pennsylvania Haptic texture toolkit (HaTT), a collection of haptic data captured from 100 surface textures together with the computational models to generate vibrations [23]. The HaTT texture models use temporal changes in force and speed as input to generate realistic vibrations that simulate interaction with real-world textures.

In parallel, researchers have designed vibrotactile patterns, known as Tactons [12], with complex frequency and amplitude patterns to deliver abstract information, metaphors, emotions, and spatial directions. For example, users could perceive various emotions via sinusoidal vibrations varying in frequency, amplitude, duration, and envelope frequency [14] or associate diverse metaphors and emotions to an open-source vibration library with more than 100 Tactons [13]. Our work builds on this literature by investigating phantom sensation illusion for complex texture waveforms generated by HaTT and demonstrating the use of TPS with texture vibrations and complex Tactons in two user applications.

B. Phantom Sensations

If multiple actuators render the same signal simultaneously, users feel a single illusory vibration between the actuators, which is known as phantom sensation (PS) [1]. The perceived location of this illusory sensation can be controlled by varying the intensity ratio of the signals given to the actuators. Thus, this illusion allows a haptic designer to deliver a sensation to a certain location (spatially static PS) or move it along a certain trajectory (spatially dynamic PS) between physical actuators. Physiological studies show that applying PS to the index and middle fingertips generates a single brain activation [24], which implies that the illusion lies between sensory perception and learned cognition. Thanks to spatial benefits of PS, many researchers investigated the rendering parameters of the illusory phantom sensations to enable the delivery of accurate and consistent spatial vibration feedback.

First, researchers have investigated various body sites for delivering PS, including head [25], whole body [3], hand [26] and fingertips [24]. Researchers have also reported that the illusion could be perceived within-body [2], out-of-body [5], and penetrating the body [4], even through the air [27]. Additionally, the illusion could be drawn along the 1-dimensional axis [4], [26] or in the 2D space [6], [28] by continuously changing the intensity ratio of the actuating stimuli, which is considered effective in providing object interactions, environmental information, assistive media for people with visual or audio impairments, and innovative experiences including magic or spells [4], [28], [29].

Second, numerous studies have assessed the motion quality and spatial accuracy of the PS. In a pioneering study of phantom sensation [1], Alles found that both linear and logarithmic rendering methods could create the illusion, while the linear method showed better localization, and the logarithmic one felt more consistent in the perceived intensity. Seo and Choi proposed a gamma-based polynomial model to generalize the synthesis framework for phantom sensations [30], which showed that the higher gamma, polynomial degrees, leads to the perception of a large moving distance in the dynamic 1D phantom sensation. Another study showed that rendering the envelope intensities based on perceptual intensity, calibrated for individual users, led to more accurate illusory locations than the prior logarithmic and linear methods [2]. These rendering methods were also modulated over time to provide apparent moving sensations among stimulating sites, for example, by changing the envelope intensity ratios between actuators in 1D [4], [26] and 2D [6], [28] configurations.

However, prior work on phantom sensations focused on a small subset of the diverse design space for vibration patterns. Most studies only tested PS with single-frequency sinusoidal signals [2], [5], [25], [26]. A study by Lee et

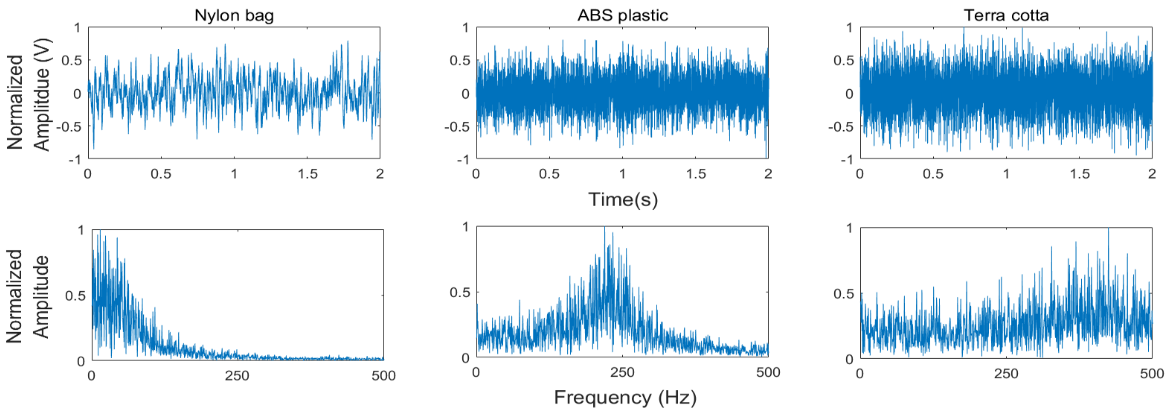

(a) Three stationary textures

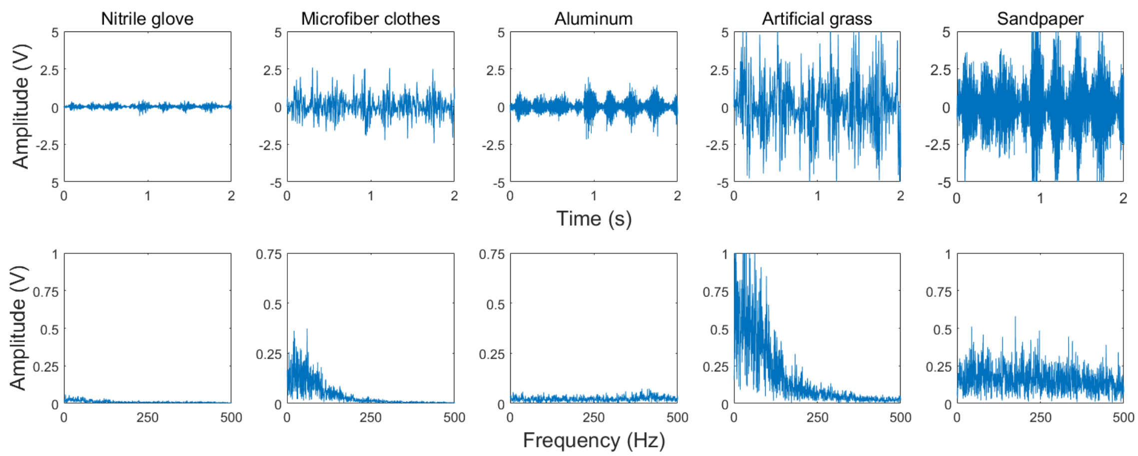

(b) Five nonstationary textures

Fig. 1. Waveform plots of (a) three stationary textures used in User Study 1. Low texture has the highest intensity peak in the low frequency range (50-200 Hz), and Mid and High textures show the highest peaks in mid (200-350 Hz) and high (350-500 Hz) frequency ranges, respectively with normalized intensities. (b) Waveform plots of five temporally nonstationary textures used in User Study 2. Texture 1 had the smallest intensity, textures 2 and 3 had intermediate intensities and texture 3 showed higher frequency components. Texture 4 includes most spectral components in the low frequency range, while texture 5 shows a wide range of spectral components with high intensities.

al. [7] implied the potential of providing PS using sinusoids with two different carrier frequencies for the two actuators. Recent attempts showed that using sinusoidal carriers with non-identical frequencies [31] or adding broadband noise [32] could induce PS, but the vibration signals with complex amplitude and frequency spectrum have not been assessed for PS rendering. Meanwhile, the tactile apparent motion illusion could create the feeling of a stroking motion on a tactile sleeve using a single texture vibration (of a leather surface) [33]. Their study validated the illusion of continuous sensation on a single body part but did not investigate user performance in identifying various textures and location information. Moreover, tactile apparent motion can only create moving sensations while PS can enable both spatially static and dynamic sensations. Building on these findings, we carefully selected complex carrier waveforms for physical textures and validated them with conventional PS rendering methods, thereby extending PS to include diverse and realistic vibrotactile feedback.

III. Textured Phantom Sensation

We designed textured phantom sensation (TPS), the phantom sensation rendered using complex waveforms of texture vibrations, by adopting methodologies of prior work on PS. As PS was designed to convey a spatially static location or dynamic sensations, our design also aimed at delivering spatially static and dynamic spatial information with additional texture information. We focused on the texture vibrations, rather than using other complex waveforms such as sounds or metaphoric Tactons because of the diverse spectral structures in textures. To improve readability, we use the terms *static* and *dynamic* to refer to spatially static and dynamic PS, respectively. These terms describe the illusory location and movement of a virtual PS stimulus. Similarly, we use *stationary* and *nonstationary* as a short form for temporally stationary and nonstationary PS, depending on whether the carrier waveform has consistent or variant envelope intensities, respectively.

A. Texture Selection

To generate texture vibration waveforms, we used the Pennsylvania haptic texture toolkit (HaTT) [23] rather than capturing texture vibrations using an accelerometer. The HaTT model can generate vibrations of pen-surface interactions from 100 different textures for a motion input, enabling us to collect and compare the vibration spectrum of textures for a controlled motion. Since most prior phantom sensations used sinusoidal vibrations with a constant intensity as a carrier waveform [1], we utilized the HaTT model in generating 1) stationary texture waveforms using a fixed motion input to generate vibrations with constant amplitude and 2) nonstationary texture waveforms with variable amplitude envelopes generated by two scratching motions.

1) Stationary Texture Vibrations: The HaTT auto-regressive moving average (ARMA) model provides a means of generating texture vibration waveforms for an arbitrary motion [23], [34]. The HaTT was designed from recordings of pen-surface interaction with motions up to 300 mm/s and 4 N of scanning speed and normal force. To obtain stationary texture waveforms, we generated 2-second vibration waveforms from 100 textures using a constant motion of 100 mm/s scanning speed and 1 N normal force. The 100 waveforms were normalized to a standard intensity level, similar to the conventional carrier signal in phantom sensation. We tried to cluster these 100 vibrations based on perceptual similarities using a voice-coil actuator (Hapcoil One; Tactile Labs). However, in our pilot study, the signals were not perceptually distinguishable for users because of their similar perceived intensities. In other words, most of them felt as noise. Thus, we examined the textures based on their spectral dissimilarity; we divided the spectrum of each waveform into three ranges of *Low* (50-200 Hz), *Mid* (200-350 Hz), and *High* (350-500 Hz) frequencies and selected texture waveforms that showed the highest energy in each bandwidth. We finally selected and used nylon bag, ABS plastic, and terra-cotta for *Low*, *Mid*, and *High* frequency bandwidths in User Study 1 (Figure 1(a)).

2) Nonstationary Texture Vibrations: We also selected non-stationary texture vibrations generated from real user motions to represent vibrations generated from real-world interaction with physical surfaces. First, we attached a 3-axis accelerometer (ADXL354cz; Analog Devices) at the top of a pen and recorded acceleration data at 10 kHz, and recorded a 60-Hz video of two scratching motions at the slow and fast speeds. Following the established procedure for texture generation, we integrated them to extract the speed of those two motions and applied real-time dimension reduction from 3D to 1D [35] and a low-pass filter of 10 Hz. Then, we selected a 2-second segment representing the intended motions well (Figure 2(a)). Finally, we computed vibration waveforms for 100 textures in the HaTT model for the two motion data using the 1 N of normal force with Gaussian noise (mean: 0; std: 0.1).

To select the most distinct vibrations, we calculated pairwise perceived dissimilarities of 100 texture vibrations using the model for the fine-texture vibrations from Bensmaïa and Hollins [36]. Then, we applied multi-dimensional scaling to the pairwise dissimilarities and visually observed their configuration in 3D (goodness-of-fit: 5.94%). Also, we applied the average linkage hierarchical clustering method to the perceived distances and determined that five clusters aligned well with the 3D space of texture data (Figure 2(b)). We found a texture from each cluster that maximizes the sum of the pairwise dissimilarities and selected nitrile gloves, microfiber clothes, aluminum, artificial grass, and sandpaper aluminum oxide as the five textures (*Tex1-5*) in User Study 2 (Figure 1(b)).

B. Rendering Algorithm for TPS

If TPS functions similarly to the previous PS, the rendering techniques would also influence the perceived positions. Thus, we adopted the prior PS rendering algorithms to validate their feasibility in textured vibrations.

In the prior literature for sinusoidal phantom sensations [1], linear rendering (*Lin*) offered better localization accuracy with inconsistent perceived intensity across the target locations. In contrast, the logarithmic (*Log*) method showed consistent perceived intensities but worse localization. Also, recent research showed that *Log* provided more linearity in perceived locations for static phantom sensations than *Lin* [5]. In moving phantom sensations, the energy-based (*Eng*) method showed stable and higher perceived intensity than the *Lin* [30] with more consistent speed [28] but shorter moving distances. To assess their spatial performance in both static and dynamic TPS, we included these three methods in our studies.

In particular, the actuators at the index and middle fingertips rendered vibration $x_i(t)$:

$$x_i(t) = A_i(t)c(t) \tag{1}$$

where $A_i(t)$ is the envelope intensity and $c(t)$ is the 2-second carrier signal or the texture waveforms in our work. Then the envelope amplitude A_i of the three methods is computed by

$$\begin{aligned} Lin: A_i(t) &= A\left(1 - \frac{d_i(t)}{D}\right), \\ Log: A_i(t) &= A\left(1 - \log_2\left(1 + \frac{d_i(t)}{D}\right)\right), \\ Eng: A_i(t) &= A\left(1 - \frac{d_i(t)}{D}\right)^{0.5} \end{aligned} \tag{2}$$

where A is the maximum amplitude, $d_i(t)$ is the current distance from the actuator i to the target location, and D is the maximum distance. We rendered the static TPS by using $D_i(t)$ to the intended location and the dynamic TPS by calculating a linear trajectory between the start and finish locations.

Next, we conducted two user studies to assess user performance with TPS (Table I).

IV. User Study 1: TPS Using Stationary Carrier Waveform

This study aimed to validate whether a texture vibration can induce phantom sensations if it has consistent envelope intensities over time (i.e., stationary TPS). We carefully selected

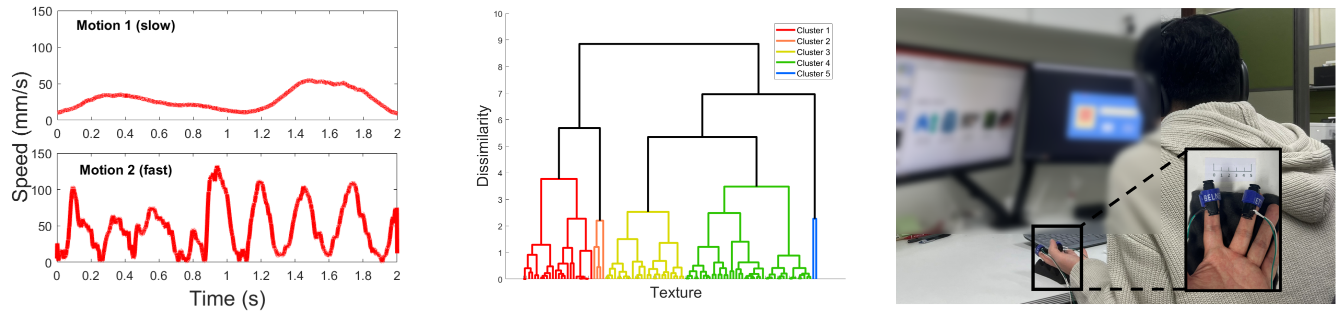

(a) Speed plots of slow and fast scratch motions

(b) Hierarchically clustered textures

(c) Setup for the user studies

Fig. 2. Plots of (a) movement speeds captured from two scratching motions over time and (b) five clusters selected from hierarchical clustering of 100 HaTT textures by pairwise dissimilarities. The (c) set up for user studies 1 and 2 showing the hand pose and actuator placement on the fingers of a participant performing the experiment.

TABLE I
DIFFERENCES OF CONDITIONS BETWEEN USER STUDY 1 AND 2.

	User Study 1	**User Study 2**
Rendering method	Linear, log, energy	Energy
Texture	Low, mid, high	Nitrile glove, microfiber clothes, aluminum, artificial grass, sandpaper
Signal	Stationary	Nonstationary
Input motion	Fixed speed	Slow, fast

three 2-second texture vibrations of nylon bag, ABS plastic, and terra-cotta using the HaTT with constant motion speed and force. For three representative PS rendering methods, we evaluated texture accuracy, spatial information, and subjective ratings of the static and dynamic TPS in a user study. Figure 2(c) shows the setup for User Study 1 and 2.

A. Methods

1) Participants: We recruited 24 participants (20 males, 4 females; 20-34 years old, Mean = 22.64, std = 3.27). None of them reported any known sensorimotor disorders, and all participants were right-handed. The experiment took about 90 minutes and the participants were paid about 24 USD. The study was approved by the Institutional Review Board (20221201-HR-69-05-04).

2) Experiment Setup: We selected the index and middle fingertips as the stimulation sites due to their sensitivity to the vibrations [36] while inducing a single activation area in the brain [24]. The literature [37] showed that physical vibration propagation from fingertip to palm is damped by 99%. Thus, the stimulus on the fingertip hardly activates mechanoreceptors on the palm [38]. To find a distance that does not induce any discomfort, we ran a pilot study (8 males, 1 female) and 6 cm was the minimum distance inducing discomfort to a user with the smallest hand size. Since the smaller distance can decrease the spatial performance of phantom sensation [3], we asked participants to keep the fingertips of their left hand 5 cm apart horizontally with the palm facing the ceiling. A real-size 5 cm ruler figure was placed on the experimental desk to visually guide participants to keep the distance.

Participants positioned their left hand on a sponge block to minimize vibration propagation and wore noise canceling headphones playing pink noise to block any auditory cues during the study. We fastened a commodity voice-coil actuator (Hapcoil-One; Tactile Labs), which has a bandwidth of 50-2000 Hz, on each fingertip using a Velcro tie. Each actuator was driven by a data acquisition board (USB-6353; National instruments) with its connected custom-made voltage follower. We compensated the actuation system with a dynamic compensation scheme as in [35] by using a 3D-accelerometer (ADXL354-cz; Analog Devices), so that each actuator could generate accelerations close to the input waveforms for 50-500 Hz bandwidth spectrum. All actuators and the accelerometer were sampled at 10 kHz.

3) Experiment Conditions: We rendered both static and dynamic TPS with three waveforms (nylon bag (*Low frequency*), ABS plastic (*Mid frequency*), and terra-cotta (*High frequency*) and three rendering methods (*Lin*, *Log*, *Eng*). Three waveforms were generated to have normalized amplitude using a constant input motion (100 mm/s scanning speed, 1 N normal force), which showed their highest spectrum peaks at 50-200, 200-350, and 350-500 Hz of their frequency ranges.

We used different conditions for spatial rendering in static and dynamic TPS. The static TPS varied five intended locations from the index (*L1*) to middle fingertips (*L5*), while *L2* to *L4* were evenly spaced between them. The perceived location accuracy was calculated by taking the distances between the perceived and intended locations regarding *L1* and *L5* as 0 and 1, respectively. For the dynamic TPS, we rendered two moving directions from *L1* to *L5* (*D15*) and *L5* to *L1* (*D51*), where the intended locations continuously changed over time.

4) Procedure: Our study consisted of four sessions: calibration, training, and two main sessions for static and dynamic TPS. Participants were verbally instructed on their posture and the whole procedure using slides before the study.

In the calibration session, the perceived intensities of the vibrations were matched for each participant to accurately provide the illusory locations. This involved two steps: texture intensity matching and actuator intensity matching. The texture intensity matching was designed to match the perceived intensities of all textures, we chose the *High* vibration as the reference because of its perceptually weakest intensity. We showed a terra-cotta image on the left and another texture image

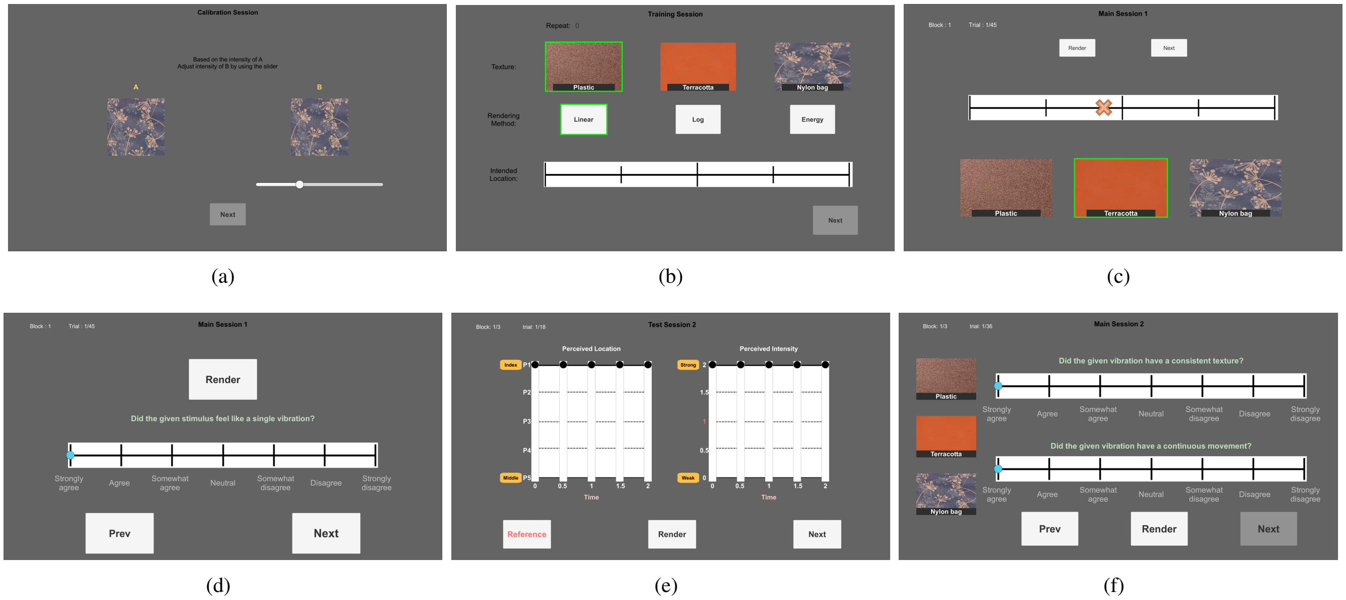

Fig. 3. User interfaces of the first study using stationary texture waveforms for the sessions: (a) calibration, (b) training, and both objective and subjective response scenes in the main sessions for the static (c, d) and dynamic (e, f) TPS. Each participant experienced these sessions in the order from (a) to (f).

of nylon bag or ABS plastic on the right, counterbalancing the order of textures across participants. Clicking on a texture image generated the relevant vibration on the index fingertip, and a participant controlled a slider to match perceptual intensities of the generated vibration to *High* vibration. The actuator intensity matching step helped equalize the stimulation intensities of both actuators. We presented the same texture images on both sides of GUI, corresponding to the index and middle fingertip actuators (Figure 3(a)). The participant then controlled a slider bar to make the vibration of both actuators feel the same.

Because phantom sensation requires a learning process for accurate location discrimination [5], we included a training session before the main session. During training, participants chose a texture, a rendering method, and an intended location by clicking on a texture image, a button, and the location along a horizontal bar, respectively. The horizontal bar included five vertical lines representing the intended *L1–L5* locations as in Figure 3(b). Each participant had to play the static TPS more than 10 times for each condition, so they experienced at least 90 static TPS vibrations during training.

The subsequent main session for static TPS consisted of three blocks, where each block included 45 trials with three textures, three rendering methods, and five intended locations, randomized without duplication. First, a participant clicked the Render button to feel a static TPS and selected the perceived location and texture by clicking on the bar and texture images (Figure 3(c)). Then, the participant could click the Next button to move to another screen and rate whether the sensation felt like a single vibration using a 7-point Likert scale from 1 (strongly disagree) to 7 (strongly agree) (Figure 3(d)). The participants could feel the static TPS and modify their three responses about location, texture, and single vibration using the Next and Prev buttons before moving to the next vibration. Also, they took a break for 5 minutes between blocks.

The dynamic TPS session consisted of three blocks with 18 trials from three textures, three rendering methods, and two moving directions. In each trial, the Render button generated dynamic TPS with a randomized order for the 18 conditions without duplication. The participant then answered perceived locations and perceived intensities over time by controlling sliders as in Figure 3(e). Participants were instructed to consider the intensity of vibration generated from the Reference button click as the reference intensity of 1. In the subjective rating scene after clicking the Next button, we collected the consistent texture perception (consistency) and continuous vibration perception (continuity) with a range of 1 (strongly disagree) and 7 (strongly agree) to the questions *“Did the given vibration have a consistent texture?”* and *“Did the given vibration have a continuous movement?”* in Figure 3(f).

B. Results

In both sessions, we discarded the first block’s data to account for the learning effect.

1) Static TPS: First, to assess the spatial information delivery, we plotted the perceived locations versus intended locations with their median values and Q1/Q3 quantiles in Figure 4(a). None of the perceived locations passed the Shapiro-Wilk normality tests, so we applied the Friedman test and the intended locations showed statistically significant differences in the perceived locations ($\chi^2(4) = 1601$, $p<0.001$). There was no significant effect of texture type or rendering method. In the post-hoc pairwise Wilcoxon tests, every intended location pair showed statistically significant differences (all $p<0.001$). Also, the average error distance for locations was 0.11. Because the spatial error passed the Shapiro-Wilk normality tests, we applied a three-way repeated measures ANOVA with factors of texture, intended location, and rendering method. Only the

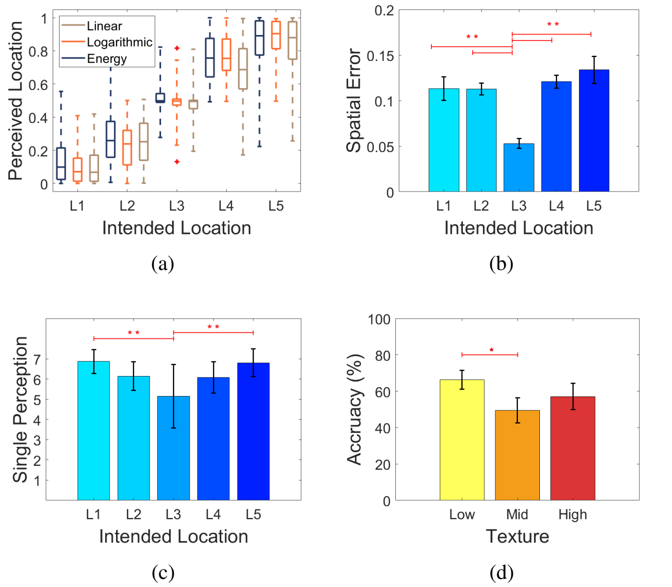

Fig. 4. Four plots of perceived locations, spatial errors, single perception ratings for each intended location, and identification accuracy for each texture.

intended location showed statistically significant differences ($F(4, 2152)$ = 10.458, p<0.01) with the average spatial error of 0.12, 0.10, 0.053, 0.11, and 0.13 for *L1-L5* respectively. Following post-hoc pairwise t-tests showed the error for *L3* was statistically significantly lower than every other intended location.

None of the single vibration ratings passed the Shapiro-Wilk normality tests, so we applied the Friedman test. As a result, only the intended location showed statistically significant differences ($\chi^2(4)$ = 37.21, p<0.001) as in Figure 4(c). In the post-hoc pairwise Wilcoxon tests, L1-L3 (W = 25, p<0.001), and L3-L5 ($W = 261$, p<0.01) showed statistically significant differences. The lowest median single vibration rating was 5.16 at L3, which is above 5, somewhat agreeable.

We also calculated the percent correctness (PC) scores for texture accuracy. The average PC scores and variances for textures *Low*, *Mid*, and *High* were 66.3 $\pm$ 0.05, 49.4 $\pm$ 0.07, and 57.1 $\pm$ 0.07, respectively (Figure 4(d)), while the average PC score across textures was 57.6 $\pm$ 0.06, which is notably higher than the probability of randomly guessing the right texture, 33.3%. All the PC scores passed the Shapiro-Wilk normality test, so we applied the three-way repeated measures ANOVA. The results showed that only textures showed statistically significant differences ($F(2, 46) = 4.69$, p<0.05). For the interaction effect, only the intended locations $\times$ textures showed a statistically significant difference ($F(8, 184) = 2.23$, p<0.05). In the post-hoc pairwise t-tests on textures, only the *Low* and *Mid* showed statistically significant differences ($t(23) = 3.08$, p<0.01).

2) Dynamic TPS: We applied the Friedman test to the perceived locations by the five temporal sampling points since they did not pass the normality tests. The perceived locations were significantly different over time ($\chi^2(4)$ = 654.09, p<0.001). The pairwise Wilcoxon signed-rank tests showed statistically significant differences for every pair (all p<0.001). The average perceived moving distances for rendering methods were 0.60, 0.08, and 0.45 for *Lin*, *Log*, and *Eng*, respectively.

To analyze the spatial rendering quality of dynamic TPS, we adopted two measures: the moving distance of the perceived location, normalized from the index to the middle fingertip as 0 to 1 (moving distance), and the variance of perceived intensities (variance) from the literature [26]. Since the moving distances did not pass the Shapiro-Wilk normality tests, we used the Friedman test to assess the effects of the three independent variables on the moving distance. The rendering method had statistically significant effects on moving distance with the average of 0.38 ($\chi^2(2)$ = 234.99, p<0.001). Post-hoc pairwise Wilcoxon rank sum tests showed *Lin* - *Log*(p<0.001) and *Log* - *Eng*(p<0.01) had significant differences. Variance also showed statistically significant differences by the rendering methods ($\chi^2(2)$ = 8.351, p<0.05) with 0.48 as average. Meanwhile, both moving distance and variance passed the normality tests for moving direction, but none of the paired t-tests showed statistically significant differences.

The consistency and continuity ratings on all factors passed the Shapiro-Wilk normality tests. The three-way repeated measures ANOVA showed that the consistency had a statistically significant effect of textures ($F(2, 34)$ = 4.25, p<0.01) without significant interactions. In the following post-hoc pairwise t-tests, *Low-High* (*Low*: 5.26 and *High*: 5.80; $t(23) = -3.47$, p<0.01) showed a statistically significant difference. The continuity had a statistically significant effect of rendering methods ($F(2, 46)$ = 8.01, p<0.01) and a significant interaction of textures, rendering methods, and moving directions ($F(4, 88)$ = 2.54, p<0.05). In the following post-hoc pairwise t-tests, *Lin-Log* (*Lin*: 5.59 and *Log*: 6.14; $t(23) = 3.29$, p<0.01) and *Log-Eng* (*Eng*: 5.86; $t(23) = 2.80$, p<0.05) were statistically different. We plotted the consistency and continuity for the rendering methods and the textures in Figure 5(g) and 5(h). While the average values were over 5 (somewhat agreeable) for both ratings for all rendering methods and textures, the *Log* showed the highest continuity in phantom sensation, and the *Mid* texture provided consistent texture perception.

We calculated the average PC scores and relevant variances of *Low*, *Mid*, and *High* as 67.7 $\pm$ 0.08, 54.1 $\pm$ 0.1, and 57.3 $\pm$ 0.08 respectively, while the overall PC score was 59.7 $\pm$ 0.09 %. The PC scores passed the Shapiro-Wilk normality tests except for the rendering method. Therefore, we applied one-way repeated measures ANOVA for the textures ($F(2, 46)$ = 2.035, $p = 0.143$), paired t-test for moving directions ($t(23) = 0.896$, $p = 0.133$), and the Friedman test for the rendering method ($\chi^2(2)$ = 4.441, $p = 0.582$), but none of the tests showed any statistically significant differences in the PC scores.

C. Discussion of Study 1 Results

We observed three main features from TPS using the stationary texture vibration. First, both static and dynamic TPS could deliver spatial information comparable to that of PS using simple sinusoidal carrier signals. Although perceived location showed no significant difference by the rendering

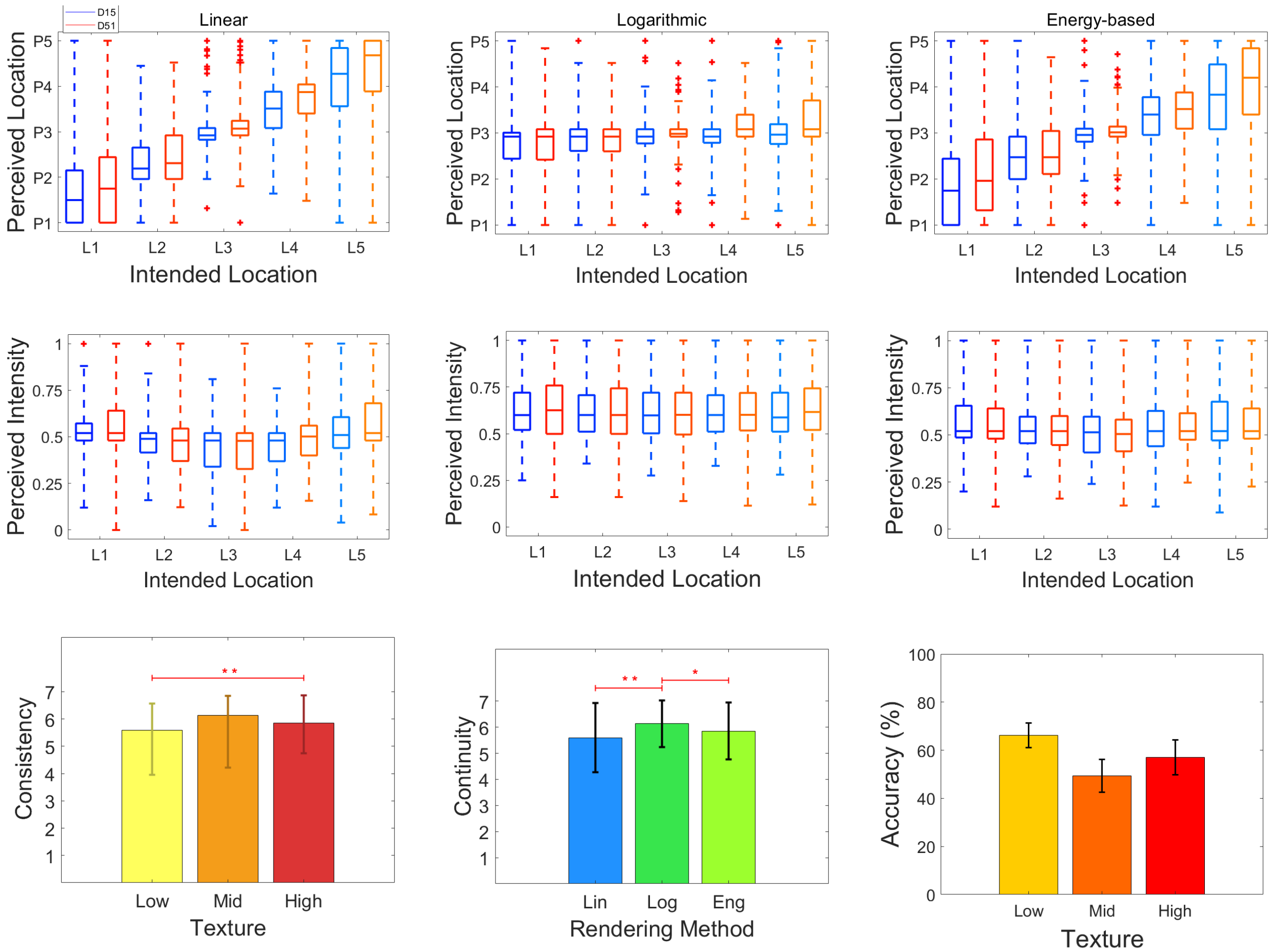

Fig. 5. Graphical representation of dynamic TPS results from User Study 1. The plots show perceived locations (top row) and intensities (middle row) over time, using linear, logarithmic, and energy-based methods. Subjective ratings are presented (bottom row) by texture and rendering method, with displaying the average texture identification accuracy for each texture.

methods in static TPS, dynamic TPS showed higher moving distance and variance in the linear method, lower in the log method, and intermediate performance in the energy method, indicating similar performance to PS [26], [30]. Therefore, TPS using stationary vibrations is capable of providing spatial information.

Second, texture identification was influenced by the texture only while it was not very accurate. In other words, the complex waveform information seems not to be affected by the phantom sensation rendering parameters in both dynamic and static phantom sensations. Our texture identification accuracies, 57.6 and 59.7% for the static and dynamic TPS, are lower than human performance on texture identification which is around 70% when providing both vibration and thermal feedback [39]. We assumed two main reasons for this confusion: 1) the training session might not be sufficient to fully account for the learning curve, and 2) the stationary waveforms generated from the constant input motion did not match real-world texture vibrations, which are generated from inconsistent force and speed, thus stationary textures were confusing to users. Specifically, participants should identify textures by solely relying on the spectral differences between three texture vibrations, not their perceived intensities, while the real-world texture perception requires more complex temporal data through various exploratory procedures [40].

Third, both static and dynamic TPS could induce illusory single vibration sensation (i.e., ratings above somewhat agreeable). For the static TPS, both *L1* and *L5* got ratings around strongly agreeable because they provided a single stimulation physically. Meanwhile, *L3* got the average rating of 5.16, indicating somewhat agreeable, as the lowest rating among the five conditions. This suggests that participants perceived the sensation as a single vibration in almost every condition. In the dynamic TPS, all of the average consistency and continuity ratings were higher than 6, so participants agreed that the single stimulation continuously moved between the fingertips and its texture was perceived as constant.

Overall results showed that TPS using the stationary texture vibrations was able to deliver spatial information, with comparable performance to the ordinary sinusoidal PS in prior literature. However, this setup was limited to using vibration envelope with constant intensities, therefore we extended TPS to more generalizable carrier signals in Study 2.

V. User Study 2: TPS Using Nonstationary Carrier Waveforms

In this study, we aimed to assess the performance of TPS for the carrier waveform generated from the input data captured by real interaction. Therefore, we generated nonstationary texture waveforms using two scratch motions with different speeds for five texture waveforms of nitrile gloves, microfiber clothes, aluminum, artificial grass, and sandpaper aluminum oxide as described in Section III-A2. In addition, we redesigned the training session to reach the learning saturation for texture identification. Then, we evaluated both spatial performance and texture accuracy of the static and dynamic TPS.

A. Method

1) Participants and Apparatus: We recruited 24 participants (16 males; 8 females; 19-33 years old, Mean = 22.85, std = 3.25) for the static and another 24 participants (13 males; 11 females; 19-32 years old, Mean = 23.21, std = 4.08) for the dynamic TPS while using the same hardware and configuration as User Study 1. None of them reported any known sensorimotor disorders and all participants were right-handed or ambidextrous. The experiment took about 50 minutes and they were paid about 15 USD in total. The study was approved by the Institutional Review Board (20240530-HR-EX-009).

2) Experiment Conditions: We rendered both static and dynamic TPS with five waveforms (nitrile gloves, microfiber clothes, aluminum, artificial grass, and sandpaper aluminum oxide; *Tex1-5*) and two user motions (*Slow* and *Fast* scratching motions). Also, we chose *Eng* for all TPS rendering in this study because it ensured spatial information delivery in both static and dynamic TPS in User Study 1. Other experiment conditions, including spatial conditions of the static and dynamic TPS, were identical to those in User Study 1 (see Table I for differences between the studies).

3) Procedure: The experiment consisted of calibration, training, and main sessions. In contrast to User Study 1, we used a between-subject design by assigning 24 participants for each of the static and dynamic TPS main sessions to limit the overall experiment duration to less than an hour considering fatigue. Before the calibration session, participants were instructed on their posture and the procedure using slides.

In the calibration session, we matched the perceived intensity for the index and middle fingertips with a 50-1000 Hz pink noise vibration. Participants adjusted the intensity of the actuator on the middle fingertip using a slider bar until the vibrations from the two actuators felt the same (Figure 6(a)).

To train participants in texture identification, we designed a two-step training session consisting of free exploration and texture learning. In the free exploration step, participants freely explored TPS by choosing the three conditions of texture, intended location, and motion and clicking the Render button as in Figure 6(b). Participants needed to experience each texture at least three times to proceed to the next step. For the multimodal recognition of texture interaction, we visualized a speed graph of the selected motion while playing a TPS simultaneously. After a participant felt the exploration was enough to pass the texture learning, they clicked the Next button to proceed.

In the texture learning step, participants had to provide ten consecutive correct answers for randomly selected textures. In each trial, participants clicked the Render button to feel a texture vibration as many times as wanted. The button also played the relevant motion video simultaneously. When the participant answered a texture among the five options and pressed the Next button, the correct texture was shown to them as in Figure 6(c). Through this positive feedback, participants could learn the textures along the learning step. We regarded ten correct answers in a row as the learning saturation on the texture identification task.

We configured two main sessions for static and dynamic TPS, but each participant was assigned to one session. The static session had three blocks, and each block included 50 trials from the five textures, two input motions, and five intended locations. In each trial, participants clicked the Render button to feel a TPS and answered its perceived location and texture by clicking the corresponding images, and pressed the Next button to proceed as shown in Figure 6(d). A 5-minute break was provided between the blocks. The dynamic session also had three blocks where each block included 20 trials with five textures, two input motions, and two intended directions. Participants could feel the vibration by clicking the Render button and answered the perceived texture and locations over time by clicking the corresponding images and controlling a slider bar as shown in Figure 6(e).

B. Results

The average number of trials for learning saturation was 96.06 across the participants (std: 62.33). We also calculated Pearson correlations between the required trials for learning saturation and individual participants' texture identification accuracy, which showed a low correlation of 0.134. All post-hoc significance levels were adjusted using Bonferroni correction.

1) Static TPS: All spatial errors, where the overall average was 0.15, passed Shapiro-Wilk normality tests, so we applied a three-way repeated measures ANOVA over texture, intended location, and input motion. The intended location and input motion did not show any statistically significant differences while texture did ($F(4, 2152) = 61.19$, $p<0.001$) and showed average spatial errors of 0.21, 0.15, 0.16, 0.13, and 0.14 for *Tex1-5*, respectively. Post-hoc t-tests showed that only nitrile gloves was significantly different from the other textures (all $p<0.001$) as shown in Figure 7.

The average PC score across textures was 67.50±0.30% while aluminum showed the lowest (58.00%) and artificial grass (73.18%) showed the highest. We applied the Friedman tests to PC scores for not passing the normality tests, and textures showed statistically significant differences ($\chi^2(4) = 21.67$, $p<0.005$) while intended location and input motion did not. Post-hoc pairwise Wilcoxon rank sum tests showed *T1 - T3* ($p<0.001$) and *T3 - T5* ($p<0.05$) had significant differences.

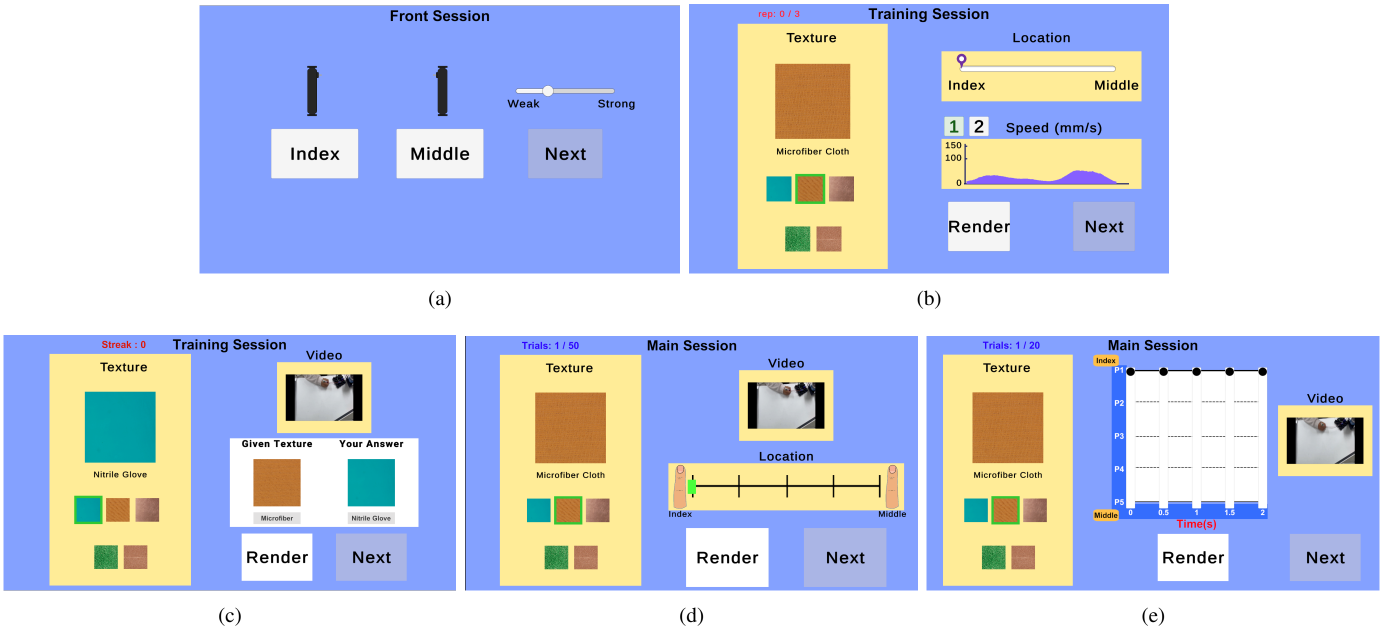

Fig. 6. User interfaces used in Study 2 for sessions of (a) calibration, (b) free exploration and (c) texture learning scenes in the training session, and (d) static and (e) dynamic main sessions.

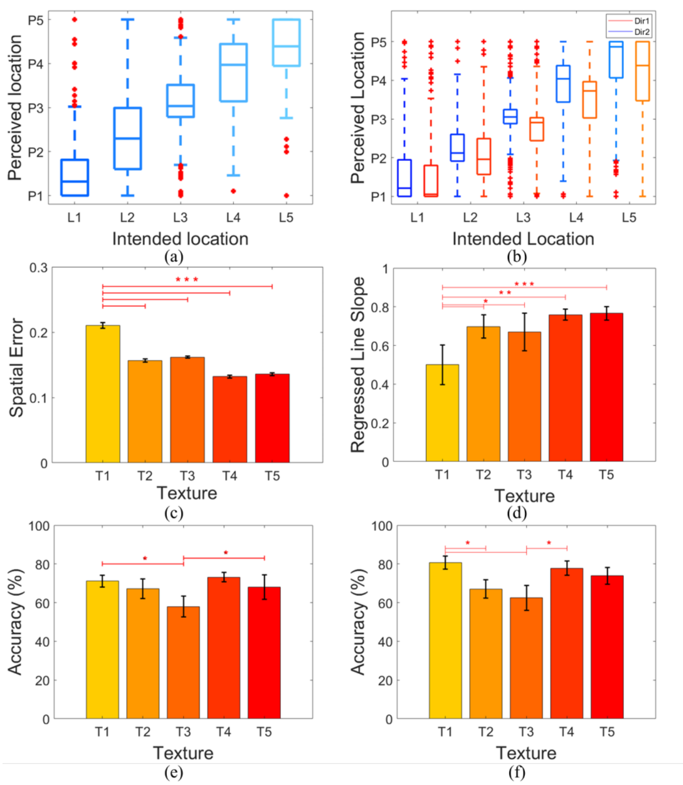

Fig. 7. Plots of Study 2 results with nonstationary TPS. The plots show perceived locations for each intended location both (a) static TPS and (b) dynamic TPS on both directions of *D15* and *D51*. Plot (c) shows spatial errors over texture in static TPS and (d) shows the average of perceived location moving distance over time in dynamic TPS. The average identification accuracies for each texture plot are described in (e) the static TPS and (f) the dynamic TPS.

2) Dynamic TPS: Similar to User Study 1, we calculated the normalized moving distance to assess the spatial performance of the dynamic sensation, but we did not calculate variance due to the inconsistent carrier intensities. Because the moving distance passed the Shapiro-Wilk normality tests, we applied a three-way repeated measures ANOVA, and statistically significant differences were found only for the texture ($F(4, 105) = 3.95$, $p<0.01$). The average moving distance was 0.68 while the lowest was observed in nitrile gloves (0.50) and the highest in sandpaper (0.77). The post-hoc t-tests also proved that only nitrile gloves showed significant differences with every other texture (Figure 7).

The average texture PC score was 72.39±0.24% while aluminum showed the lowest (62.50%) and artificial grass the highest (77.84%). Because PC scores did not pass the Shapiro-Wilk normality tests, we applied the Friedman test for texture ($\chi^2(4) = 24.3$, $p<0.001$) and following post-hoc pairwise Wilcoxon rank sum tests showed *T1 - T2*, *T1 - T3*, and *T3 - T4*(all $p<0.05$) had significant differences.

C. Discussion of Study 2 Results

First, when using the nonstationary carrier waveforms, both static and dynamic TPS delivered spatial information while showing lower accuracy than the consistent carrier waveforms. We assume that the inconsistent waveforms provided irregular perceived intensities by their changes in frequency bandwidths and envelope intensities over time because the perceived intensity varies by the frequency shifts [41]. Our observation underlying relationship between the total energy of texture and perceived location also supports this assumption. From the spectrum plots for five textures (Figure 1(b)), textures with lower spectral intensities resulted in higher spatial errors. Because perceived intensity follows the logarithmic mapping from the physical stimulation, the frequency-amplitude shift at the low physical intensity significantly affects the perceived intensities. This relationship also appeared in dynamic TPS, where the moving distance of nitrile gloves was significantly lower than the other textures.

Meanwhile, texture identification performance with multimodal (motion video and vibration) representation increased with the dynamic compared to the static TPS by 4.89%p.

This increase suggests that the multimodal representation of the texture vibrations might have positively affected the texture recognition in the dynamic TPS. Moreover, the average identification accuracy was around 70%, which is similar to the human performance of texture identification for the thermo-vibration feedback [39]. Therefore, TPS seems to have the potential to deliver the information included in nonstationary textures if it is provided with multimodal feedback.

VI. Applications of TPS

We expect TPS rendering to be beneficial for various end-user applications. In this section, we share our experiences when we showcased two demonstrations of TPS, which helped us collect qualitative user feedback in an interactive scenario.

A. Two Hands-on Demonstrations

We held our first nonstationary TPS demo after User Study 1. The demo configuration was the same as in User Study 1, but we let users interact with texture surfaces using a pen attaching an accelerometer (Figure 8(a)). Therefore, users could generate and feel TPS with the carrier waveform from unconstrained motions using the real-time dimensional reduction algorithm [35]. Users could control conditions the static or the dynamic TPS, rendering methods, and a target stimulation location or direction for better interactivity. Most users reported that they felt a distinct single illusory sensation at a static location or along a moving trajectory while emphasizing the motion clarity of the dynamic TPS. The responses were aligned with our results in User Study 1, for example, *"The dynamic TPS with Log was not clear in the moving sensation while that with Lin felt a salient motion."* Also, the comment of *"The dynamic TPS of rough materials felt as more clear in location and moving sensation than soft textures,"* reflects the importance of carrier vibration energy in the delivery PS.

Our second demo, conducted after the User Study 2, let participants play a brick-breaking game to verify the user experiences induced by TPS in an actual game, not in a controlled experiment as shown in Figure 8(b). Users controlled a bar using a mouse to bounce balls back, while the mouse grasping hand attached actuators on the index and middle fingertips. We implemented a static TPS with impulse carrier signals according to the three textures of the bar [22] at the location where the ball collides with the bar. Also, when a user caught an item, the dynamic TPS was provided corresponding to the texture of the bar and the acquired item. Most of the users responded that the haptic feedback was harmonic to the given situation. Specifically, they reported that the temporally decaying material vibrations felt realistic and the co-located stimulation with PS provided an immersive experience.

B. Potential Application Examples

Beyond our demonstrations, TPS can enhance user experiences across various applications. For example, offering safe interactions with complex material properties or the dynamics of fluid in VR. It can also augment senses by allowing users to perceive the size, position, distance, and texture of distant objects, potentially aiding visually impaired individuals. Furthermore, TPS enables beyond-real interactions in VR gaming, creating tactile feedback for magical actions and nuanced visual effects. The feasibility of combining complex vibration patterns with phantom sensations opens avenues for exploring TPS on other body parts and expanding its application scope.

VII. Discussion

We confirmed that TPS can deliver spatial information with carrier signals using both stationary and nonstationary waveforms, while the texture identification rate reached the known human performance of using a single vibrotactile channel. In this section, we summarize key implications found in our user studies.

By using the wide-band carrier waveform, both static and dynamic TPS can provide spatial information. Phantom sensation is known to mainly provide spatial information using a small number of vibration actuators, and the literature reported its performances while using the sinusoidal carrier signals. In our studies, stationary TPS showed 0.11 of average spatial error in static location delivery, which was smaller than 0.15 for the nonstationary TPS in all five locations. Referring to the previous work on 2D static phantom sensations, the sinusoidal carrier showed 0.1–0.2 and 0.02–0.1 Euclidean errors at the edge and center of the 2D coordinate, respectively. The stationary waveforms showed 0.12 and 0.13 at *P1* and *P5* while *P3* induced 0.053 of spatial errors, which aligns with the sinusoidal waveform. Therefore, the static spatial information seems to mainly depend on the constant envelope intensity of the carrier waveform.

Meanwhile, for the dynamic phantom sensation, moving distance and intensity variance were measured for spatial information as described in the literature [26]. In the literature, four-second sinusoidal phantom sensation yielded 0.56 and 0.25 of moving distance values for the linear and log methods, respectively. In our results, stationary TPS showed 0.60, 0.08, and 0.43 of moving distance for the linear, log, and energy-based methods for the 2-second duration, where the linear method showed similar perceived position changes to the sinusoidal dynamic PS while the log method barely showed any movement. Notably, the energy-based method applied with the nonstationary waveforms showed 0.68 of moving distance. In summary, TPS seems applicable for providing both static and dynamic spatial information.

TPS can deliver complex texture information at a single location and along a trajectory. Both studies showed 58.6 and

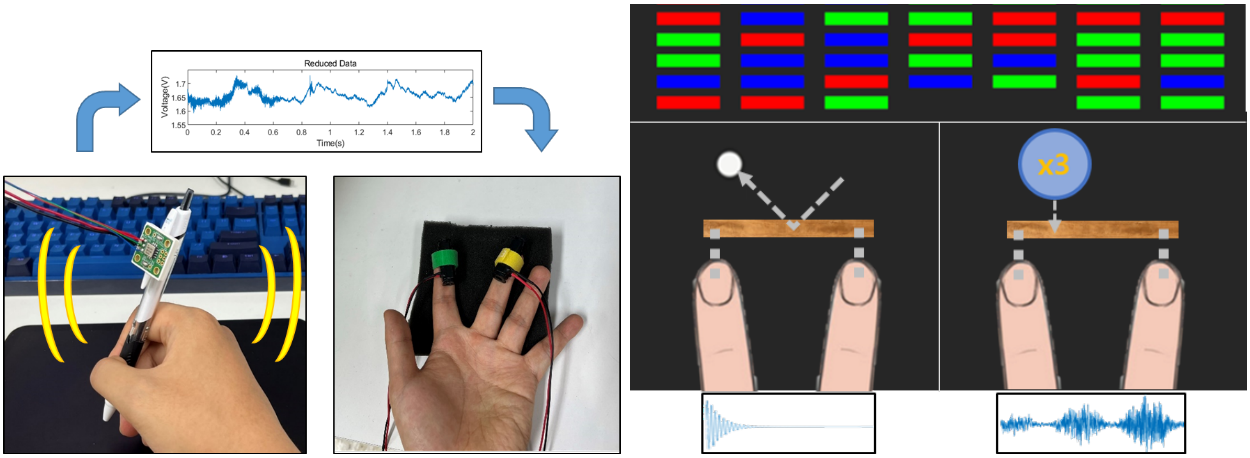

Fig. 8. Two demonstrations utilizing both static and dynamic TPS. (left) Users could feel TPS of the carrier waveform which was captured from the users' pen-surface interactions in real time. (right) In a brick-break game, users could feel the static TPS for the collision between a ball and a bar and the dynamic TPS for catching an item.

69.9% of texture accuracy in percent correct scores. Despite the low scores, it is known that a single vibration signal is not capable of supporting highly accurate identification of textures, especially with passive touch; the texture identification with the vibro-thermal feedback led to about 70.83% of correct identification by a human operator. Even though we could not find any statistically significant differences in texture accuracy, dynamic TPS showed higher average texture accuracy in both cases. We assume that the Pacinian channel might sensitively respond to the envelope intensity changes of the dynamic TPS because it rapidly adapts to the sensation [36]. Referring to this work, TPS seems capable of delivering the same level of texture information as a single vibration actuator does, especially in using nonstationary waveforms.

Multimodal representation of TPS using the nonstationary waveforms enhances the information delivery included in the complex waveform. Although we cannot directly compare the two studies due to different designs, we showed the gradient increment of the texture identification accuracy while using nonstationary waveforms. One big difference comes from the inclusion of motion videos to provide the context of texture vibration, which might help users relate the TPS to the textures. The motion videos showed the hand movement where its input motion data was given to the HaTT Model for texture waveform generation, therefore the intensities and spectral changes were in sync with the videos. Also, the same scratching motion induced different frequency bandwidths and intensities, which generated nonstationary and distinct waveforms. We assume that the participants could identify textures by relating the spatiotemporal data to the input motion. Therefore, TPS with the appropriate visual motions would enhance the understanding of the interaction context which helps to recognize the texture information.

Based on our user studies and demonstrations, we identified three main directions where TPS could be further studied. First, though we validated TPS with and without visual cues in User Study 1 and 2, respectively, they were not directly compared. We have a weak assumption that the TPS without visual cues might not be accurate in both spatial information and event identification. Therefore, TPS needs to be validated in VR scenarios requiring feedback for the events occurring out of a user avatar's sight (e.g., another user scratches the avatar's back with a finger). The other direction is integrating the TPS with Tactons, which are the tactile patterns for delivering diverse information from emotions to metaphors. If the integration works, then the already-diverse design space of Tactons would gain another dimension in delivering tactile information to users, especially in VR environments.

VIII. Conclusion

We showed that the phantom sensation carrying complex waveform could deliver both texture and spatial information. In User Study 1, we first designed a phantom sensation study using the stationary texture vibration waveforms generated from a fixed normal force and speed, and the spatial accuracy was comparable to the sinusoidal PS while the texture accuracy was not satisfactory. We also validated TPS for texture waveforms generated from the real motion data with multimodal representation in User Study 2, which slightly decreased spatial accuracy but was comparable to the human performance of texture identification with single-channel vibrations. Additionally, we found that the energy of texture mainly affected the spatial accuracy in both static and dynamic TPS. We hope that our work will enable other researchers to further explore PS rendering methods with complex carrier waveforms on various body parts to deliver realistic and rich spatial vibrotactile feedback.

IX. Acknowledgement

This work was funded by the National Research Foundation of Korea (NN32030), Korea Creative Content Agency (GM17290), and the National Science Foundation (#2339707), and VILLUM FONDEN (VIL50296). We also thank reviewers for their input on this work.

REFERENCES

[1] D. S. Alles, "Information transmission by phantom sensations," *IEEE transactions on man-machine systems*, vol. 11, no. 1, pp. 85–91, 1970.

[2] G. Yun, S. Oh, and S. Choi, "Seamless phantom sensation moving across a wide range of body," in *2019 IEEE world haptics conference (WHC)*. IEEE, 2019, pp. 616–621.

[3] H. Elsayed, M. Weigel, F. Müller, M. Schmitz, K. Marky, S. Günther, J. Riemann, and M. Mühlhäuser, "Vibromap: Understanding the spacing of vibrotactile actuators across the body," *Proceedings of the ACM on Interactive, Mobile, Wearable and Ubiquitous Technologies*, vol. 4, no. 4, pp. 1–16, 2020.

[4] J. Kim, S. Oh, C. Park, and S. Choi, "Body-penetrating tactile phantom sensations," in *Proceedings of the 2020 CHI Conference on Human Factors in Computing Systems*, 2020, pp. 1–13.

[5] G. Park and S. Choi, "Tactile information transmission by 2d stationary phantom sensations," in *Proceedings of the 2018 CHI conference on human factors in computing systems*, 2018, pp. 1–12.

[6] J. Seo and S. Choi, "Edge flows: Improving information transmission in mobile devices using two-dimensional vibrotactile flows," in *2015 IEEE World Haptics Conference (WHC)*. IEEE, 2015, pp. 25–30.

[7] J. Lee, Y. Kim, and G. J. Kim, "Rich pinch: Perception of object movement with tactile illusion," *IEEE transactions on haptics*, vol. 9, no. 1, pp. 80–89, 2015.

[8] I. Hwang, J. Seo, and S. Choi, "Perceptual space of superimposed dual-frequency vibrations in the hands," *PloS one*, vol. 12, no. 1, p. e0169570, 2017.

[9] K. J. Kuchenbecker, J. Romano, and W. McMahan, "Haptography: Capturing and recreating the rich feel of real surfaces," in *Robotics Research: The 14th International Symposium ISRR*. Springer, 2011, pp. 245–260.

[10] A. M. Okamura, M. R. Cutkosky, and J. T. Dennerlein, "Reality-based models for vibration feedback in virtual environments," *IEEE/ASME transactions on mechatronics*, vol. 6, no. 3, pp. 245–252, 2001.

[11] J. Lee and S. Choi, "Real-time perception-level translation from audio signals to vibrotactile effects," in *Proceedings of the SIGCHI Conference on Human Factors in Computing Systems*, 2013, pp. 2567–2576.

[12] K. E. MacLean, "Foundations of transparency in tactile information design," *IEEE Transactions on Haptics*, vol. 1, no. 2, pp. 84–95, 2008.

[13] H. Seifi, K. Zhang, and K. E. MacLean, "Vibviz: Organizing, visualizing and navigating vibration libraries," in *2015 IEEE World Haptics Conference (WHC)*. IEEE, 2015, pp. 254–259.

[14] Y. Yoo, T. Yoo, J. Kong, and S. Choi, "Emotional responses of tactile icons: Effects of amplitude, frequency, duration, and envelope," in *2015 IEEE World Haptics Conference (WHC)*. IEEE, 2015, pp. 235–240.

[15] R. W. Lindeman, R. Page, Y. Yanagida, and J. L. Sibert, "Towards full-body haptic feedback: the design and deployment of a spatialized vibrotactile feedback system," in *Proceedings of the ACM symposium on Virtual reality software and technology*, 2004, pp. 146–149.

[16] J. Ryu, J. Chun, G. Park, S. Choi, and S. H. Han, "Vibrotactile feedback for information delivery in the vehicle," *IEEE Transactions on Haptics*, vol. 3, no. 2, pp. 138–149, 2010.

[17] I. Sarakoglou, N. Garcia-Hernandez, N. G. Tsagarakis, and D. G. Caldwell, "A high performance tactile feedback display and its integration in teleoperation," *IEEE Transactions on Haptics*, vol. 5, no. 3, pp. 252–263, 2012.

[18] D. Valkov and L. Linsen, "Vibro-tactile feedback for real-world awareness in immersive virtual environments," in *2019 IEEE Conference on Virtual Reality and 3D User Interfaces (VR)*. IEEE, 2019, pp. 340–349.

[19] W. McMahan, J. M. Romano, A. M. A. Rahuman, and K. J. Kuchenbecker, "High frequency acceleration feedback significantly increases the realism of haptically rendered textured surfaces," in *2010 IEEE Haptics Symposium*. IEEE, 2010, pp. 141–148.

[20] E. D. Gomez, R. Aggarwal, W. McMahan, K. Bark, and K. J. Kuchenbecker, "Objective assessment of robotic surgical skill using instrument contact vibrations," *Surgical endoscopy*, vol. 30, no. 4, pp. 1419–1431, 2016.

[21] S. Merchel, M. E. Altinsoy, and M. Stamm, "Touch the sound: audio-driven tactile feedback for audio mixing applications," *Journal of the Audio Engineering Society*, vol. 60, no. 1/2, pp. 47–53, 2012.

[22] G. Park and S. Choi, "A physics-based vibrotactile feedback library for collision events," *IEEE Transactions on Haptics*, vol. 10, no. 3, pp. 325–337, 2016.

[23] H. Culbertson, J. Unwin, and K. J. Kuchenbecker, "Modeling and rendering realistic textures from unconstrained tool-surface interactions," *IEEE transactions on haptics*, vol. 7, no. 3, pp. 381–393, 2014.

[24] L. M. Chen, R. M. Friedman, and A. W. Roe, "Optical imaging of si topography in anesthetized and awake squirrel monkeys," *Journal of Neuroscience*, vol. 25, no. 33, pp. 7648–7659, 2005.

[25] M. Kim, A. Abdulali, and S. Jeon, "Rendering vibrotactile flow on backside of the head: Initial study," in *2018 IEEE Games, Entertainment, Media Conference (GEM)*. IEEE, 2018, pp. 1–250.

[26] J. Seo and S. Choi, "Initial study for creating linearly moving vibrotactile sensation on mobile device," in *2010 IEEE Haptics Symposium*. IEEE, 2010, pp. 67–70.

[27] A. Bellicha, A. Trujillo-Leon, and W. Bachta, "Phantom sensation: When the phantom escapes the bounds of the actuators and the end-point is sensed in the air," in *2019 IEEE World Haptics Conference (WHC)*. IEEE, 2019, pp. 91–96.

[28] A. Israr and I. Poupyrev, "Tactile brush: drawing on skin with a tactile grid display," in *Proceedings of the SIGCHI Conference on Human Factors in Computing Systems*, 2011, pp. 2019–2028.

[29] S. Ahn, G. Jin, G. Park, and J.-H. Hong, "Enhancing video experiences for dhh individuals through sound-inspired motion caption-based spatiotemporal tacton," *IEEE Transactions on Haptics*, 2025.

[30] J. Seo and S. Choi, "Perceptual analysis of vibrotactile flows on a mobile device," *IEEE transactions on haptics*, vol. 6, no. 4, pp. 522–527, 2013.

[31] K. Shim and G. Park, "Matching performance of 2d phantom sensations with visual motions," in *2024 IEEE Haptics Symposium (HAPTICS)*. IEEE, 2024, pp. 403–408.

[32] R. Kirchner, R. Rosenkranz, B. G. Sousa, S.-C. Li, and M. E. Altinsoy, "Phantom illusion based vibrotactile rendering of affective touch patterns," *IEEE Transactions on Haptics*, vol. 17, no. 2, pp. 202–215, 2023.

[33] H. Culbertson, C. M. Nunez, A. Israr, F. Lau, F. Abnousi, and A. M. Okamura, "A social haptic device to create continuous lateral motion using sequential normal indentation," in *2018 IEEE haptics symposium (HAPTICS)*. IEEE, 2018, pp. 32–39.

[34] H. Culbertson, J. J. L. Delgado, and K. J. Kuchenbecker, "One hundred data-driven haptic texture models and open-source methods for rendering on 3d objects," in *2014 IEEE haptics symposium (HAPTICS)*. IEEE, 2014, pp. 319–325.

[35] G. Park and K. J. Kuchenbecker, "Objective and subjective assessment of algorithms for reducing three-axis vibrations to one-axis vibrations," in *2019 IEEE World Haptics Conference (WHC)*. IEEE, 2019, pp. 467–472.

[36] S. Bensmaïa and M. Hollins, "Pacinian representations of fine surface texture," *Perception & psychophysics*, vol. 67, pp. 842–854, 2005.

[37] B. Dandu, Y. Shao, and Y. Visell, "Rendering spatiotemporal haptic effects via the physics of waves in the skin," *IEEE Transactions on Haptics*, vol. 14, no. 2, pp. 347–358, 2020.

[38] N. Tummala, Y. Shao, and Y. Visell, "Spatiotemporal organization of touch information in tactile neuron population responses," in *2023 IEEE World Haptics Conference (WHC)*. IEEE, 2023, pp. 183–189.

[39] E. Kerr, T. M. McGinnity, and S. Coleman, "Material classification based on thermal and surface texture properties evaluated against human performance," in *2014 13th International Conference on Control Automation Robotics & Vision (ICARCV)*. IEEE, 2014, pp. 444–449.

[40] S. J. Lederman and R. L. Klatzky, "Extracting object properties through haptic exploration," *Acta psychologica*, vol. 84, no. 1, pp. 29–40, 1993.

[41] K. Parsons and M. Griffin, "Whole-body vibration perception thresholds," *Journal of sound and Vibration*, vol. 121, no. 2, pp. 237–258, 1988.